Nonlinear extension of the x-ray diffraction enhanced imaging

Anton Maksimenko[a)]
High Energy Accelerator Research Organization (KEK), 1-1 Oho, Tsukuba, Ibaraki 305-0801, Japan

(Received 29 September 2006; accepted 9 March 2007; published online 12 April 2007)

Diffraction enhanced imaging is the analyzer-based x-ray imaging technique which allows extraction of the refraction and absorption contrasts from two images taken on the opposite sides of the rocking curve of the analyzer. It is widely used in different fields of science. However, the information provided by the method is qualitative rather than quantitative. This happens because either side of the rocking curve is approximated as a line. One can overcome this problem of considering the rocking curve instead of the approximation. This letter is dedicated to the implementation of this idea and includes theoretical background and experimental validation. © *2007 American Institute of Physics*. [DOI: 10.1063/1.2721378]

When an x ray penetrates through an object it deflects on its boundaries and inner inhomogeneities. It also absorbs and scatters inside the object so that the outgoing beam holds information on the object structure. The information is recorded in the distributions of intensity and deflection. In contrast to the intensity, the measurement of the deflections is a complicated procedure since the refraction coefficient for the hard x ray is very close to unity: $\tilde{n} \equiv 1-n \sim 10^{-5}-10^{-7}$. It leads to the very small deflections of the same order. The experimental system which can visualize such small deflections usually includes an analyzing device placed between the object and the detector (see Refs. 1–7). The contrast obtained under this condition is a mixture of the absorption and refraction components. In 1997 Chapman *et al.* presented the diffraction enhanced imaging (DEI) method[2] which can separate the components using two images taken on either side of the rocking curve (RC) of the analyzing crystal. Although the images obtained via the DEI are informative, the quantitative analysis is suspicious since the accuracy of the method is very limited. However, higher accuracy is required for the recent applications of the refraction contrast [for example, refraction-based computed tomography[8–16] (CT)]. Since the invention of the DEI, different modifications of the method were presented.[6,10,13,17] These modifications strongly improve the accuracy of the method but they require more images to be recorded for the data process. Depending on the method, 17–28 images are needed. It strongly exceeds the two images required by the original DEI. This fact limits potential applications of these methods. In this letter we would like to present one more modification of the DEI which can significantly improve the accuracy and extend the sensitivity ranges still using only two images.

Similar to the original DEI,[2] the experimental system consists of collimating and analyzing crystals, an object placed between them, and a detector after the analyzer. The images are taken on each side of the RC with the analyzer set to Θ_L and Θ_H from the Bragg angle [points L and H in Fig. 1(a), respectively]. The intensity diffracted by the analyzer in each position can be expressed as follows:

$$I_{L,H} = I_R R(\Theta_{L,H} + \alpha), \tag{1}$$

where α is the refraction angle of the x ray passed through the object, I_R is the apparent absorption intensity, and $R(\Theta)$ is the RC of the analyzer. The DEI utilizes two-term Taylor expansion of the RC in the above equation: $R(\Theta_{L,H}+\alpha) \approx R(\Theta_{L,H}) + \alpha(dR/d\Theta)(\Theta_{L,H})$. This converts Eq. (1) to the linear system with the solution given by Eqs. (6a) and (6b) from Ref. 2. However, the Taylor approximation limits the applicability and introduces unwanted error. It is illustrated in Fig. 1(a) where the RC is presented together with the approximation. One can note that the approximation is well adequate in the region of smaller refractions, but the accuracy decreases with the increase of the refraction. In order to overcome this problem one can use the RC instead of the linear approximation. This may be considered as the nonlinear extension of the DEI method and can be referred to as the extended DEI (EDEI). Combining Eq. (1) we can exclude member I_R from:

$$\frac{I_L - I_H}{I_L + I_H} = \frac{R_L(\alpha) - R_H(\alpha)}{R_L(\alpha) + R_H(\alpha)} \equiv F(\alpha), \tag{2}$$

where we used the denotation $R_{L,H}(\alpha) = R(\Theta_{L,H}+\alpha)$. The combination used above limits possible values of the function $F(\alpha)$ to the range $[-1;1]$ [see full line in Fig. 1(b)]. This function is monotonously growing in the region between two extreme points. Assuming that the refraction angle does not

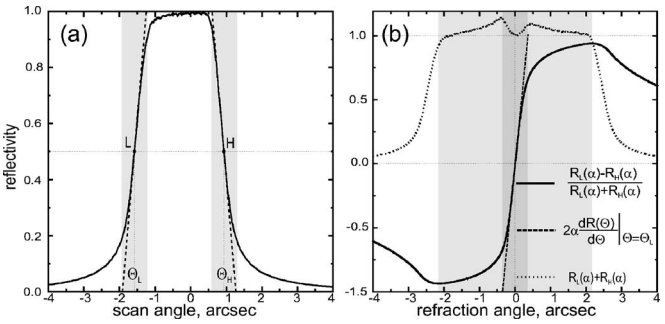

FIG. 1. (a) RC of the analyzer (full line) and its two-term Taylor approximation (dashed line). (b) Full line represents function $F(\alpha)$ defined in Eq. (2), dashed line is its Taylor approximation, and dotted line shows the ratio of the absorption contrasts calculated via EDEI and DEI methods. The gray boxes show the region of applicability of the DEI (darker) and EDEI (lighter).

[a)]Electronic mail: antonmx@post.kek.jp

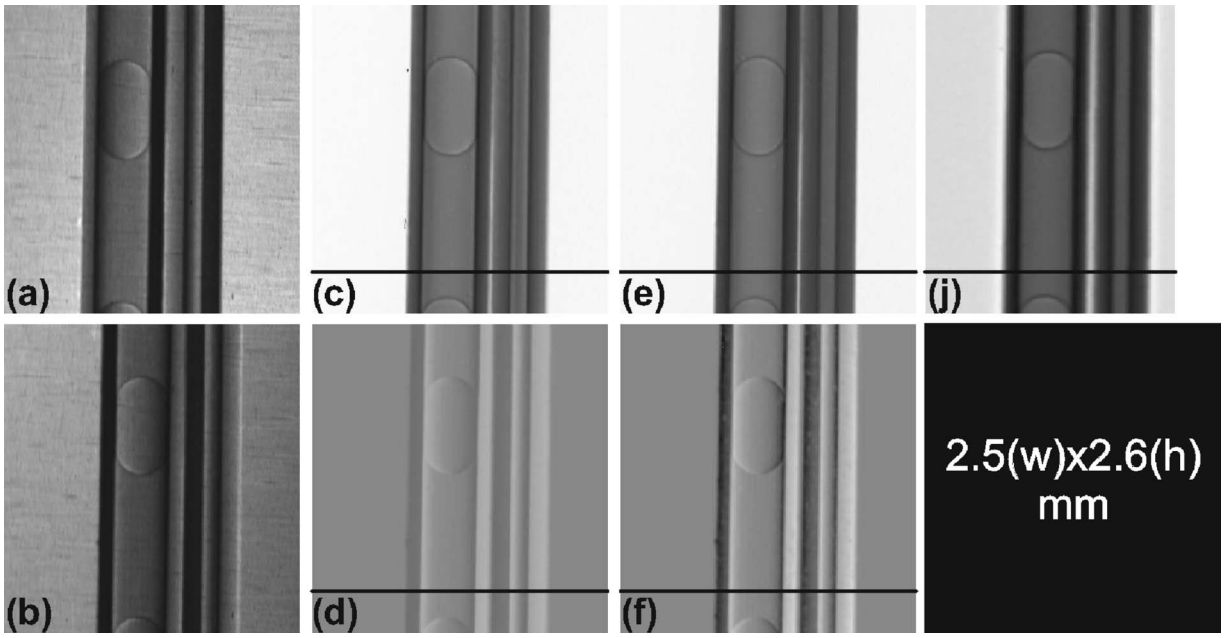

FIG. 2. Originally acquired images in the (a) L and (b) H points of the RC. Absorption contrasts calculated by the (c) DEI and (e) EDEI. [(d) and (f)] Refraction contrasts obtained via the DEI and EDEI, respectively. (j) Absorption contrast at the same object-to-detector distance recorded directly without the analyzer. The profiles of the slices shown with black horizontal lines are presented in Fig. 3.

exceed this region, one may construct a single-valued inverse function:

$$\alpha = F^{-1}\left(\frac{I_L - I_H}{I_L + I_H}\right). \tag{3}$$

Then the refraction angle α calculated from the above equation can be used in the expression for the absorption intensity I_R:

$$I_R = \frac{I_L + I_H}{R_H(\alpha) + R_L(\alpha)}. \tag{4}$$

The theory described above shows that the applicability ranges of the EDEI may be much wider than those of the DEI. It can be clearly understood taking into account the origins of the limits. In the case of DEI the limits are defined by the divergence used in the Taylor expansion. They are shown in Fig. 1(a) as the gray box. In the EDEI case the limits are defined by the region where the function $F(\alpha)$ is monotonously growing [see the gray box in Fig. 1(b)]. Comparison shows that the EDEI's applicability ranges are almost six times wider under the same experimental conditions. Moreover, the EDEI method provides more flexibility in the choice of the angles Θ_L and Θ_H. The DEI requires the angles Θ_L and Θ_H to be set to the inflection point of the RC. In practice they are defined by the condition $R(\Theta)=0.5$. Contrastingly, the EDEI does not impose so strong a requirement. The angles may be chosen reasoning from the desired shape of the function $F(\alpha)$.

We performed the experiment to illustrate this theoretical approach. We used the vertical wiggler beamline BL14B at the Photon Factory, KEK, Japan. Both monochromator and analyzer were Si(220) crystals with the asymmetry angles of 9.5° and −9.5°, respectively. The photon energy used in the experiment was 11.7 keV. Under these conditions the Bragg angle $\Theta_B=16.0°$ and asymmetry factors of the monochromator and the analyzer are 0.26 and 3.8, respectively. The RC of the analyzer is presented in Fig. 1(a). The sample under investigation consisted of two AlO_2 pipes partly filled with oil. The outer and inner diameters of the larger pipe were 0.6 and 0.4 mm, respectively, while those of the smaller pipe were 0.4 and 0.11 mm in sizes. The object-to-analyzer and analyzer-to-detector distances were 320 and 430 mm, respectively. The positions of the analyzing crystal on the low- and high-angle sides were chosen from the condition $R(\Theta_L)=R(\Theta_H)=0.5$. The images of the object are pre-

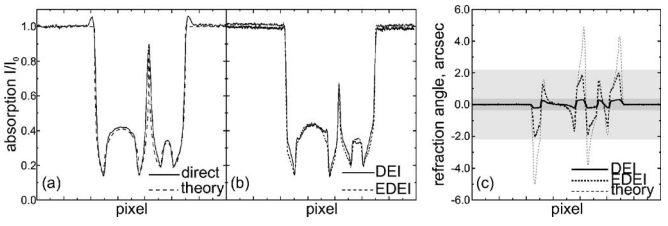

FIG. 3. Profiles of the contrasts depicted in Fig. 2. (a) Theoretical expectation of the absorption profile and profile of Fig. 2(j). (b) Profiles of absorption contrasts in Figs. 2(c) (dashed line) and 2(e) (full line). (c) Profiles of refraction contrasts in Figs. 2(f) (dotted line) and 2(d) (full line) as well as theoretical prediction (dashed line). The gray boxes denote the limits of applicability of the EDEI (lighter) and DEI (darker).

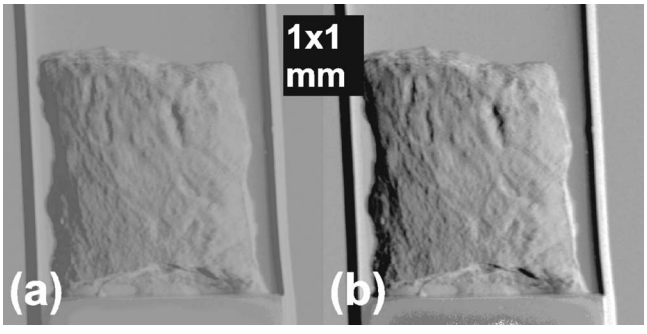

FIG. 4. Refraction contrasts of the breast cancer sample extracted via (a) DEI and (b) EDEI methods. The vertical stripes on each side of the sample are the sample holder—a plastic tube.

sented in Figs. 2(a) and 2(b) for the L and H points, respectively. The initially recorded images were 3.8 times wider due to the asymmetrically cut analyzer. Here they are shown resized to match the scales. The contrasts were processed in accordance with the DEI and EDEI approaches. The results of the process are depicted in Fig. 2. The absorption and refraction contrasts obtained via the DEI are shown in Figs. 2(c) and 2(d), respectively, while the corresponding pair of contrasts the resulted from the EDEI can be found in Figs. 2(e) and 2(f). The black lines in the images denote the profiles which are presented in Fig. 3. Another sample tested in the experiment was the real breast cancer part. The sample had a semicylindrical shape of approximately 3×3 mm^2 in size. The images of this sample were taken under the same experimental condition. The extracted refraction contrasts are shown in Fig. 4. The images are similar to Fig. 4(b) but taken at different rotations of the sample composing the CT set. This set was reconstructed and the results were published and discussed in Ref. 15.

One can note that the difference between the absorption contrasts extracted by the methods is not significant. We can understand this fact by comparing the expression for the absorption in Eq. (4) with the one used in the DEI. In our experiment we had $R'(\Theta_L)=-R'(\Theta_H)$ which reduces Eq. 6(b) from Ref. 2 to $I_R=I_L+I_H$. Then the ratio between the absorption intensities calculated by the DEI and EDEI methods is equal to $R_L(\alpha)+R_L(\alpha)$ [dotted line in Fig. 1(b)]. This ratio never exceeds 20% within the region of possible deflections. This relatively small difference explains the similarity of the absorption contrasts. The situation is totally different in the case of the refraction contrasts. The refraction contrasts of both samples extracted via the EDEI are much sharper and more intense. Also the EDEI profile of the first sample is much closer to that theoretically expected [see Fig. 3(c)]. Once again we can explain this fact by comparing corresponding expressions in the EDEI [Eq. (3)] and DEI [Eq. (6a) in Ref. 2]. The analysis of the latter equation shows that the DEI can be considered as a particular case of the EDEI with $F(\alpha)=2\alpha R'(\Theta_L)$ [dashed line in Fig. 1(b)]. The comparison of two curves $F(\alpha)$ emphasizes that the difference between the refractions calculated via the two methods may exceed 500% in the region of higher deflections. The EDEI is accurate within 10% error unless the refraction angle stays in the region twice narrower than the sensitivity boundaries. Therefore, the EDEI must be preferable in the fields where further data processing is performed (for example, refraction-based CT). One can also note that the first sample we used in the experiment provides deflections outside the applicability region [see the theoretically predicted profile in Fig. 3(c)]. This choice of sample allows us to check what happens when the refraction is too strong. The predicted and calculated refractions coincide well unless the refraction does not exceed the limits, otherwise higher deflections are cut out. This happens because the function $F(\alpha)$ is not uniquely defined outside the limits and the ambiguity is solved for the benefit of the values within the limits.

In conclusion we can say that the EDEI is the important extension of the DEI. It dramatically improves the accuracy of the results, makes the sensitivity limits wider at the same experimental conditions, and provides additional flexibility in the experimental setup. Among the disadvantages of the method we may point out higher process time. Calculation of the point on the line needed in the DEI is computationally much cheaper. In practice the EDEI proved to be approximately six times cheaper. Therefore the EDEI can be considered as a reasonable compromise between fast but inaccurate DEI and advanced but complicated multiimaging techniques.[6,10,13,17]

The author would like to acknowledge the members of his working group who helped him in the preparation of the letter: Masami Ando, Hiroshi Sugiyama, and Eiko Hashimoto. This work was partly supported by the Japan Society for the Promotion of Science.

[1] V. Ingal and E. Beliaevskaya, J. Phys. D **28**, 2314 (1995).
[2] D. Chapman, W. Thomlinson, R. E. Johnston, D. Washburn, E. Pisano, N. Gmür, Z. Zhong, R. Menk, F. Arfelli, and D. Sayers, Phys. Med. Biol. **42**, 2015 (1997).
[3] P. Cloetens, W. Ludwig, and J. Baruchel, Appl. Phys. Lett. **75**, 2912 (1999).
[4] M. Ando, K. Hyodo, H. Sugiyama, A. Maksimenko, W. Pattanasiriwisawa, K. Mori, J. Roberson, E. Rubenstein, Y. Tanaka, J. Chen, D. Xian, and Z. Xiaowei, Jpn. J. Appl. Phys., Part 1 **41**, 4742 (2002).
[5] A. Bravin, J. Phys. D **36**, A24 (2003).
[6] M. N. Wernick, O. Wirjadi, D. Chapman, Z. Zhong, N. P. Galatsanos, Y. Yang, J. G. Brankov, O. Oltulu, M. A. Anastasio, and C. Muehleman, Phys. Med. Biol. **48**, 3875 (2003).
[7] M. Ando, K. Yamasaki, C. Ohbayashi, H. Esumi, K. Hyodo, H. Sugiyama, G. Li, A. Maksimenko, and T. Kawai, Jpn. J. Appl. Phys., Part 2 **44**, L998 (2005).
[8] F. A. Dilmanian, Z. Zhong, B. Ren, X. Y. Wu, L. D. Chapman, I. Orion, and W. C. Thomlinson, Phys. Med. Biol. **45**, 933 (2000).
[9] K. M. Pavlov, C. M. Kewish, J. R. Davis, and M. J. Morgan, J. Phys. D **34**, A168 (2001).
[10] I. Koyama, Y. Hamaishi, and A. Momose, AIP Conf. Proc. **705**, 1283 (2004).
[11] M. Wernick, J. Brankov, D. Chapman, Y. Yang, C. Muehleman, Z. Zong, and M. A. Anastasio, Proc. SPIE **5535**, 369 (2004).
[12] A. Maksimenko, M. Ando, H. Sugiyama, and T. Yuasa, Appl. Phys. Lett. **86**, 124105 (2005).
[13] J. G. Brankov, M. N. Wernick, Y. Yang, J. Li, C. Muehleman, Z. Zhong, and M. A. Anastasio, Med. Phys. **33**, 278 (2006).
[14] P. P. Zhu, J. Y. Wang, Q. X. Yuan, W. X. Huang, H. Shu, B. Gao, T. D. Hu, and Z. Y. Wub, Appl. Phys. Lett. **87**, 264101 (2005).
[15] E. Hashimoto, A. Maksimenko, H. Sugiyama, K. Hyodo, D. Shimao, T. Yuasa, Y. Nishino, T. Ishikawa, K. Mori, Y. Arai, K. Hirano, and M. Ando, Proc. SPIE **6142**, 369 (2006).
[16] Zhi-Feng Huang, Ke-Jun Kang, Zheng Li, Pei-Ping Zhu, Qing-Xi Yuan, Wan-Xia Huang, Jun-Yue Wang, Di Zhang, and Ai-Min Yu, Appl. Phys. Lett. **89**, 041124 (2006).
[17] E. Pagot, P. Cloetens, S. Fiedler, A. Bravin, P. Coan, J. Baruchel, J. Härtwig, and W. Thomlinson, Appl. Phys. Lett. **82**, 3421 (2003).